

## Vortices in superconducting $\text{Ba}(\text{Fe}_{0.93}\text{Co}_{0.07})_2\text{As}_2$ studied via small-angle neutron scattering and Bitter decoration

M. R. Eskildsen,<sup>1,\*</sup> L. Ya. Vinnikov,<sup>2</sup> T. D. Blasius,<sup>1,†</sup> I. S. Veshchunov,<sup>2</sup> T. M. Artemova,<sup>2</sup> J. M. Densmore,<sup>1</sup> C. D. Dewhurst,<sup>3</sup> N. Ni,<sup>4</sup> A. Kreyssig,<sup>4</sup> S. L. Bud'ko,<sup>4</sup> P. C. Canfield,<sup>4</sup> and A. I. Goldman<sup>4</sup>

<sup>1</sup>*Department of Physics, University of Notre Dame, Notre Dame, Indiana 46556, USA*

<sup>2</sup>*Institute of Solid State Physics, Russian Academy of Sciences, Chernogolovka, Moscow Region 142432, Russia*

<sup>3</sup>*Institut Laue-Langevin, 6 Rue Jules Horowitz, F-38042 Grenoble, France*

<sup>4</sup>*Department of Physics and Astronomy and Ames Laboratory, Iowa State University, Ames, Iowa 50011, USA*

(Received 22 December 2008; published 3 March 2009)

We present small-angle neutron scattering (SANS) and Bitter decoration studies of the superconducting vortices in  $\text{Ba}(\text{Fe}_{0.93}\text{Co}_{0.07})_2\text{As}_2$ . A highly disordered vortex configuration is observed at all measured fields and is attributed to strong pinning. This conclusion is supported by the absence of a Meissner rim in decoration images obtained close to the sample edge. The field dependence of the magnitude of the SANS scattering vector indicates vortex lattice domains of (distorted) hexagonal symmetry, consistent with the decoration images which show primarily sixfold coordinated vortex domains. An analysis of the scattered intensity shows that this decreases much more rapidly than expected from estimates of the upper critical field, consistent with the large degree of disorder.

DOI: [10.1103/PhysRevB.79.100501](https://doi.org/10.1103/PhysRevB.79.100501)

PACS number(s): 74.25.Qt, 74.70.Dd, 61.05.fg

The recent discovery of superconductivity in  $\text{LaFeAsO}$ ,<sup>1</sup> with critical temperatures increasing to 38 K upon doping or 43 K when subjected to hydrostatic pressure,<sup>2,3</sup> has sparked a strong interest in these materials. However, synthesis, and especially the growth of single crystals, of these materials has proven to be a challenge. It was therefore a significant step forward when it was reported that the intermetallic compound  $\text{BaFe}_2\text{As}_2$  could be rendered superconducting by doping either K on the Ba site,<sup>4,5</sup> or Co on the Fe site.<sup>6,7</sup> This discovery enabled the possibility of obtaining large high-quality single crystals grown from flux.

Here we report on combined small-angle neutron scattering (SANS) and high-resolution Bitter decoration studies of the vortices in superconducting  $\text{Ba}(\text{Fe}_{0.93}\text{Co}_{0.07})_2\text{As}_2$ .<sup>7</sup> The SANS measurements show a ring of scattering, indicating a highly disordered vortex configuration, and with a rocking curve extending beyond the measurable range. This result is confirmed and extended to lower fields by the Bitter decoration images. The disordering is attributed to strong vortex pinning, which is supported by the absence of a Meissner rim in decoration images obtained close to the sample edge. The field dependence of the magnitude of the SANS scattering vector indicates vortex lattice domains of (distorted) hexagonal symmetry. An analysis of the scattered intensity due to the vortices shows a rapid decrease with increasing applied magnetic field, significantly exceeding what would be expected based on estimates of the upper critical field.

SANS measurements were performed on a 260 mg single crystal of  $\text{Ba}(\text{Fe}_{0.93}\text{Co}_{0.07})_2\text{As}_2$ . The single crystal used in the SANS experiment was grown from a FeAs/CoAs mixture and had a critical temperature  $T_c=21$  K with a relatively narrow transition width  $\Delta T_c=2$  K measured by dc magnetization.<sup>7</sup> The experiment was performed at the D22 SANS instrument at the Institut Laue-Langevin. Incident neutrons with wavelength  $\lambda_n=6-14$  Å and wavelength spread of  $\Delta\lambda_n/\lambda_n=10\%$  were used, and the diffraction pattern collected by a position sensitive detector. Measurements were performed at 2 K in horizontal magnetic fields up to

810 mT, applied at angle of  $5^\circ-10^\circ$  to the  $c$  axis to reduce background scattering from crystallographic defects. All vortex measurements were done at 2 K, following a field-cooling procedure. Background measurements obtained at  $25 \text{ K} > T_c$  were subtracted from the data.

The high-resolution Bitter decoration experiments were performed on a  $\text{Ba}(\text{Fe}_{0.93}\text{Co}_{0.07})_2\text{As}_2$  single crystal, on an as grown surface perpendicular to the  $c$  axis, for applied magnetic fields between 1 and 32 mT along the  $c$  axis and following a field-cooling procedure. The crystal surface was flat and shiny except in areas with growth steps. The initial sample temperature was 1.7 K, increasing to 5–6 K at the end of the decoration process. The sample was subsequently imaged using a scanning electron microscope in the second electron emission regime to locate the islands of iron particles which had decorated the sample at the vortex positions.<sup>8</sup>

Figures 1(a)–1(d) shows vortex diffraction patterns obtained at four different applied magnetic fields between 810 and 450 mT. For all the magnetic fields investigated, a disordered vortex “lattice” (VL) is observed, evident by a “powder-diffraction” ring of scattering instead of well-defined Bragg peaks. It is reasonable to suppose that the disordering of the VL is caused by pinning of vortices to defects in the sample. Nonetheless, the ring of scattering indicates that short-range order persists, with small-ordered VL domains randomly oriented with respect to one another. The intensity variation around the rings of scattering suggests the existence of maxima along the horizontal and vertical axes corresponding to the  $\{100\}$  directions, indicating a VL preferred orientation even if it is insufficient to cause the coalignment of all domains.

Scattering from the vortices is expected at a radial distance from the center of the detector which is proportional to the VL scattering vector,  $q$ . As the magnetic field, and hence the vortex density, decreases the average intervortex spacing increases as  $a \propto (\phi_0/B)^{1/2}$ , where  $\phi_0=h/2e=20.7 \times 10^4 \text{ T } \text{Å}^2$  is the flux quantum. Lowering the field we

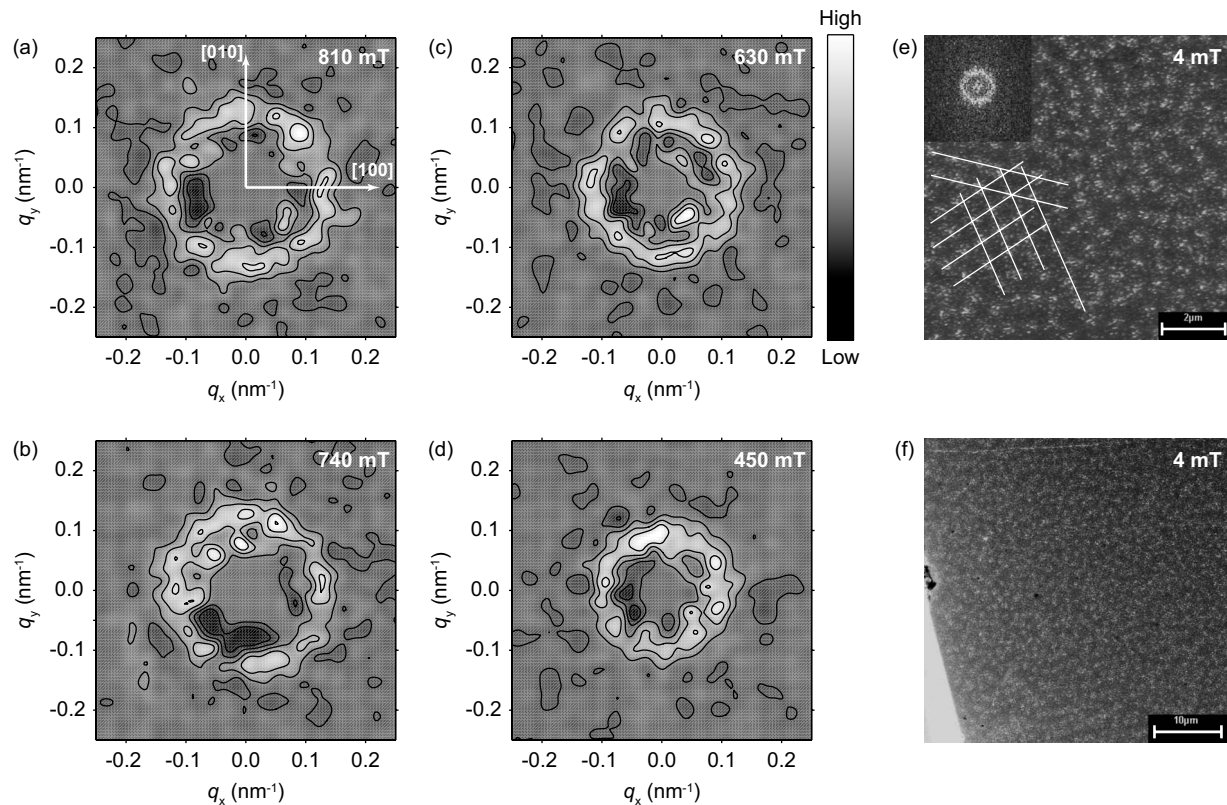


FIG. 1. Vortex imaging in  $\text{Ba}(\text{Fe}_{0.93}\text{Co}_{0.07})_2\text{As}_2$  by [(a)–(d)] SANS and [(e) and (f)] Bitter decoration. The SANS vortex diffraction patterns were obtained at 2 K and applied fields of (a) 810, (b) 740, (c) 630, and (d) 450 mT, following a field-cooling procedure. A quantitative intensity scale is shown in panel (c). The field was applied at a  $5^\circ$ – $10^\circ$  angle with respect to the crystalline  $c$  axis to reduce background scattering from crystallographic defects. For all four fields data were collected at a single (centered) orientation of the magnetic field with respect to the neutron beam direction, and background measurements obtained at  $25\text{ K} > T_c$  were subtracted. The data is smoothed and the central part of the detector is masked off. The decoration images were obtained in a magnetic field of 4 mT in the center of sample (e) and in the vicinity of sample edge (f). Small-ordered domains can be observed as indicated in (e). The inset to (e) shows the Fourier transform of the entire decoration image.

therefore expect the ring of scattering to shrink since  $q \propto 2\pi/a \propto (B/\phi_0)^{1/2}$  decreases. This is clearly seen in Figs. 1(a)–1(d), confirming that the scattering is indeed due to the superconducting vortices.

Results of Bitter decoration measurements obtained in a magnetic field 4 mT are shown in Figs. 1(e) and 1(f). A close inspection of the decoration image in Fig. 1(e) reveals primarily sixfold coordinated vortices, as well as the existence of small well-ordered domains with a size of  $\sim 5$  vortex spacings. However, no long-range orientational order is established, as evident from the Fourier transform of the decoration pattern image shown in the insert. The Fourier transform is directly comparable to the diffraction patterns in Figs. 1(a)–1(d). Combined with the SANS results this confirms that the disorder is predominantly orientational and longitudinal (along the vortices or field direction) but not  $\Delta d$ -disorder (vortex spacing). Similar results were obtained at fields as low as 1 mT and as high as 32 mT. Computing the average area associated with each vortex in a 1 mT decoration image (not shown), we find a magnetic flux per vortex of  $(21 \pm 1) \times 10^4\text{ T \AA}^2$ , in agreement with  $\phi_0$ . Further proof of strong bulk pinning is the absence of a Meissner rim (low vortex density region) in the decoration image shown in Fig. 1(f), which was obtained near the edge of the sample.<sup>9</sup>

Our observation of a disordered vortex arrangement is consistent with recent reports of scanning tunneling microscopy (STS) imaging in  $\text{Ba}(\text{Fe}_{0.93}\text{Co}_{0.07})_2\text{As}_2$ .<sup>10</sup> However, compared to small-scale direct space imaging such as STS, our results demonstrate that the disordering is a bulk effect, not restricted to the sample surface or isolated regions.

The field dependence of the scattering vector is also evident from Fig. 2, which show the radial intensity distribution corresponding to each of the diffraction patterns in Figs. 1(a)–1(d).

Fitting each radial intensity curve to a Gaussian it is possible to obtain a quantitative measure of both the magnitude of the scattering vector and the scattered intensity. Furthermore the full width at half maximum of the fits yield  $\Delta q/q \approx 0.3$ , which is  $\sim 50\%$  larger than the experimental resolution and consistent with scattering from small-ordered domains of size  $\sim (\pi\Delta q/q)^{-1}$ , corresponding to a few VL spacings in agreement with the decoration results. If one considers a rhombic VL unit cell as shown in the insets to Fig. 3(b), the scattering vector is given by  $q = 2\pi(B/\phi_0 \sin \beta)^{1/2}$ , where  $\beta$  is the opening angle. Here  $\beta = 60^\circ$  (or  $120^\circ$ ) corresponds to a hexagonal VL, and  $\beta = 90^\circ$  corresponds to a square VL. Figure 3(a) shows the measured scattering vector as a function of applied magnetic field,

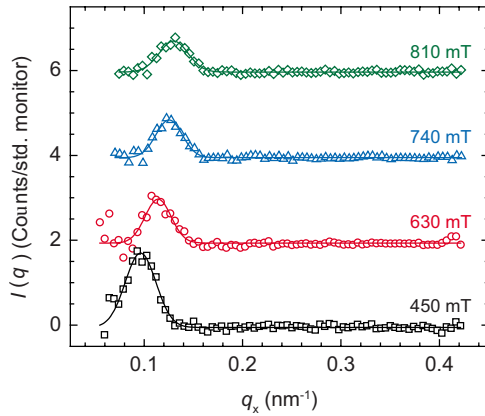


FIG. 2. (Color online) Radial intensity distribution for the four diffraction patterns in Figs. 1(a)–1(d). The curves have been offset by 2 (Counts/std. monitor) for clarity. Also shown is a Gaussian fit to the data at each field.

compared to that expected for, respectively, a square and a hexagonal VL. With the exception of a single data point, all the measured scattering vectors fall between  $q_{\text{hex}}$  and  $q_{\text{sq}}$  although it is closer to the former. This is consistent with the observation of primarily sixfold coordinated vortices in the decoration images. Figure 3(b) shows the measured scatter-

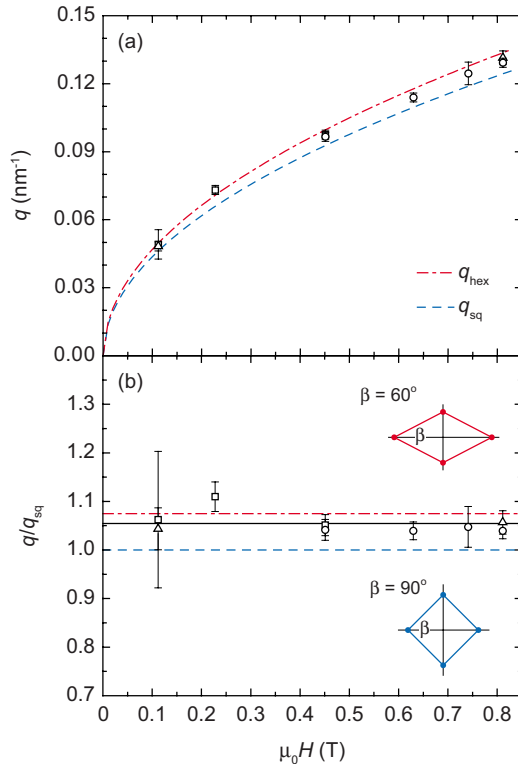


FIG. 3. (Color online) Comparison of (a) the measured scattering vector and (b) the ratio  $q/q_{\text{sq}}$  to that expected for a square (dashed lines) and a hexagonal (dot-dashed lines) vortex lattice. The solid line in panel (b) is the average  $q/q_{\text{sq}}=1.055$ . The different symbols correspond to measurements performed at different neutron wavelength,  $\lambda_n$ .

ing vector normalized to  $q_{\text{sq}}$ . Within the error bars, no field dependence of the normalized scattering vector is observed over the measured field range.

While a hexagonal VL is expected for an isotropic material, it is also well known that most tetragonal superconductors possess enough anisotropy to stabilize a square VL above a certain magnetic field.<sup>11–15</sup> The origin of the anisotropy can arise either from the Fermi surface of a given material coupled with nonlocal electrodynamics<sup>16</sup> or it can be due to anisotropic pairing in the superconducting state.<sup>17</sup> Given that a near hexagonal VL symmetry is observed in Ba(Fe<sub>0.93</sub>Co<sub>0.07</sub>)<sub>2</sub>As<sub>2</sub> at all the measured fields, it is tempting to conclude that the superconducting state in the basal plane of this material is highly isotropic. However, it has been shown that, at least in the case of a square VL stabilized by a Fermi-surface anisotropy, the critical field for the transition to the square symmetry depends strongly on the so-called nonlocality range, which decreases with increasing levels of impurities (decreasing mean free path).<sup>18</sup> From our results it is not possible to conclude which mechanism is responsible for the hexagonal VL in Ba(Fe<sub>0.93</sub>Co<sub>0.07</sub>)<sub>2</sub>As<sub>2</sub>.

We now turn to the integrated scattered intensity obtained from the Gaussian fits to the radial intensity distribution as shown in Fig. 2. From a measurement of the absolute reflectivity,  $R$ , it is possible to determine the VL form factor by

$$|F(q)|^2 = \frac{16\phi_0^2 q}{2\pi\gamma^2\lambda_n^2 t} R, \quad (1)$$

where  $\gamma=1.91$  is the neutron gyromagnetic ratio and  $t$  is the sample thickness.<sup>19</sup> However, to put the form factor on an absolute scale, the scattered intensity from the vortices should be integrated as the sample, and magnetic field, are rotated with respect to the incoming neutron beam, causing the reflections to cut through the Ewald sphere. In the case of Ba(Fe<sub>0.93</sub>Co<sub>0.07</sub>)<sub>2</sub>As<sub>2</sub> scattering from the vortices showed no measurable change in intensity even for rotations of several degrees. This indicates that the high degree of disorder found in the basal plane is also present along the direction of the vortices, causing them to deviate substantially from the applied field direction. In this regard the results in Ba(Fe<sub>0.93</sub>Co<sub>0.07</sub>)<sub>2</sub>As<sub>2</sub> are reminiscent of those obtained on CaC<sub>6</sub>.<sup>20</sup> Our results are consistent with the report of Prozorov *et al.*<sup>21</sup> of a highly disordered vortex phase in Ba(Fe<sub>0.93</sub>Co<sub>0.07</sub>)<sub>2</sub>As<sub>2</sub>, based on the analysis of transport measurements.

Our inability to measure a proper rocking curve means that a determination of the form factor on an absolute scale is not possible. On the other hand, if we assume a constant rocking curve width, the radial integrated intensity will be proportional to  $|F(q)|^2$ . Due to the strong pinning in the sample, and relatively small field range investigated, we believe that this is a reasonable assumption. The form factors obtained in this fashion are shown in Fig. 4 on a logarithmic scale. Here it is important to stress that even though the absolute magnitude of  $|F(q)|^2$  is not known, the relative field dependence can still be determined. The data are well fitted by an exponential field dependence as shown by the solid line in Fig. 4.



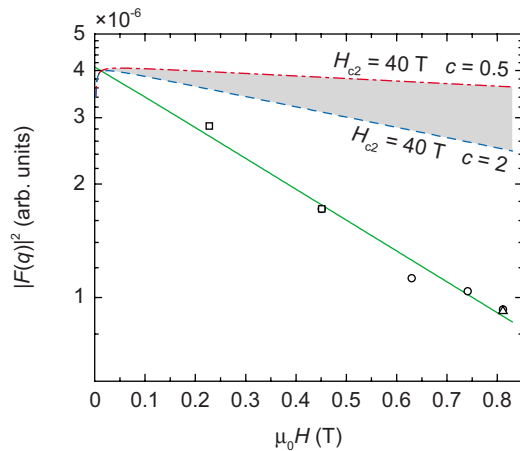


FIG. 4. (Color online) Field dependence of the vortex scattered intensity shown on a logarithmic scale. The different symbols correspond to measurements performed at different neutron wavelength,  $\lambda_n$ . The solid line is an exponential fit to the data with a slope of  $-0.82$  ( $1/T$ ). The dashed and dot-dashed lines show the form factor calculated using the London model [Eq. (2)] with  $c = 2$  and  $1/2$  respectively, and  $H_{c2} = 40$  T.

Several models exist for the form-factor field dependence. By far the simplest is based on the London model, extended by a Gaussian cutoff to take into account the finite extent of the vortex cores,

$$F(q) = \frac{B}{1 + (q\lambda)^2} e^{-c(\xi q)^2}. \quad (2)$$

Here  $\lambda$  and  $\xi$  are, respectively, the penetration depth and coherence length and the constant  $c$  is typically taken to be between  $1/4$  and  $2$ .<sup>22</sup> Even though more realistic models for the form factor are available, the London model is deemed adequate for the following discussion since the SANS measurements were performed at  $T \approx 0.1T_c$  and  $H \ll H_{c2}$ . For simplicity we will also assume a square vortex lattice for the following analysis. It should be stressed that neither of these

choices affect the following discussion in any significant fashion. For all fields studied  $(q\lambda)^2 \gg 1$  and since  $q^2 = (2\pi)^2 B / \phi_0$  the form factor in Eq. (2) decreases exponentially with increasing magnetic field.

As shown in Fig. 4, the measured intensity is indeed well fitted by an exponential decrease. If we use the fitted slope to estimate the superconducting coherence length we obtain  $\xi = 10$  nm. Here we have used  $c = 0.5$  which in the past has been found to yield reasonable values for  $\xi$  in other materials.<sup>23</sup> However, this value of  $\xi$  is roughly 3.5 times higher than expected from the extrapolated upper critical field of  $\approx 40$  T at 2 K.<sup>7</sup> For comparison the  $H_{c2}$  corresponding to this “measured”  $\xi$  is only 3.3 T, more than an order of magnitude less than the measured upper critical field. The difference is emphasized in Fig. 4, which shows the range of the calculated form factor (shaded area) corresponding to the real  $H_{c2}$  and the two extreme values of  $c$ . From this it is clear that the measured form factor falls off much faster than expected. We believe that this rapid decrease in the scattered intensity is due to the high degree of disorder of the “vortex lattice” in  $\text{Ba}(\text{Fe}_{0.93}\text{Co}_{0.07})_2\text{As}_2$ . This result is indicative of the existence of a vortex glass or randomly oriented domains of a Bragg glass, consistent with the results of Klein *et al.*<sup>24</sup>

In summary, we have performed SANS and Bitter decoration studies of the vortices in superconducting  $\text{Ba}(\text{Fe}_{0.93}\text{Co}_{0.07})_2\text{As}_2$ . At all the fields investigated, the results showing a highly disordered vortex configuration were observed, most likely due to strong pinning in this material. Further measurements at higher fields and temperatures should be carried out to fully explore the vortex phase diagram in this and related compounds.

This work was supported by the National Science Foundation through Grants No. DMR-0804887 (M.R.E. and J.M.D.) and No. PHY-0552843 (T.D.B.). L.Y.V. and I.S.V. thank the Russian Foundation for Basic Research Grant No. RFBR 07-02-00174 for support. Work at the Ames Laboratory was supported by the U.S. Department of Energy, Basic Energy Sciences under Contract No. DE-AC02-07CH11358.

\*eskildsen@nd.edu

†Also at University of Michigan.

<sup>1</sup>Y. Kamihara *et al.*, *J. Am. Chem. Soc.* **130**, 3296 (2008).

<sup>2</sup>H. Takahashi *et al.*, *Nature (London)* **453**, 376 (2008).

<sup>3</sup>X. H. Chen *et al.*, *Nature (London)* **453**, 761 (2008).

<sup>4</sup>M. Rotter *et al.*, *Phys. Rev. Lett.* **101**, 107006 (2008).

<sup>5</sup>N. Ni *et al.*, *Phys. Rev. B* **78**, 014507 (2008).

<sup>6</sup>A. S. Sefat *et al.*, *Phys. Rev. Lett.* **101**, 117004 (2008).

<sup>7</sup>N. Ni *et al.*, *Phys. Rev. B* **78**, 214515 (2008).

<sup>8</sup>L. Ya. Vinnikov *et al.*, in *The Real Structure of High- $T_c$  Superconductors*, edited by V. Sh. Shekhtman (Springer-Verlag, Berlin, Heidelberg, 1993), p. 89.

<sup>9</sup>L. Ya. Vinnikov *et al.*, *Physica C* **308**, 99 (1998).

<sup>10</sup>Y. Yin *et al.*, arXiv:0810.1048, *Phys. Rev. Lett.* (to be published).

<sup>11</sup>M. R. Eskildsen *et al.*, *Phys. Rev. Lett.* **78**, 1968 (1997).

<sup>12</sup>L. Ya. Vinnikov *et al.*, *Phys. Rev. B* **64**, 024504 (2001).

<sup>13</sup>M. R. Eskildsen *et al.*, *Phys. Rev. Lett.* **90**, 187001 (2003).

<sup>14</sup>S. P. Brown *et al.*, *Phys. Rev. Lett.* **92**, 067004 (2004).

<sup>15</sup>M. Yethiraj *et al.*, *Phys. Rev. B* **72**, 060504(R) (2005).

<sup>16</sup>V. G. Kogan *et al.*, *Phys. Rev. B* **55**, R8693 (1997).

<sup>17</sup>M. Ichioka *et al.*, *Phys. Rev. B* **59**, 8902 (1999).

<sup>18</sup>P. L. Gammel *et al.*, *Phys. Rev. Lett.* **82**, 4082 (1999).

<sup>19</sup>D. K. Christen *et al.*, *Phys. Rev. B* **15**, 4506 (1977).

<sup>20</sup>R. Cubitt *et al.*, *Phys. Rev. B* **75**, 140516(R) (2007).

<sup>21</sup>R. Prozorov *et al.*, *Phys. Rev. B* **78**, 224506 (2008).

<sup>22</sup>See A. Yaouanc *et al.*, *Phys. Rev. B* **55**, 11107 (1997).

<sup>23</sup>M. R. Eskildsen *et al.*, *Phys. Rev. Lett.* **79**, 487 (1997).

<sup>24</sup>T. Klein *et al.*, *Nature (London)* **413**, 404 (2001).